Title: Relative water content consistently predicts drought mortality risk in seedling populations with different morphology, physiology, and times to death.

Authors: Gerard Sapes[1,2] and Anna Sala[1]

[1] Division of Biological Sciences, University of Montana, Missoula, MT 59812, USA.

[2] Department of Ecology, Evolution, and Behavior; University of Minnesota, Saint Paul, Minnesota 55108, USA.

Corresponding Author:

Gerard Sapes (gsapes@umn.edu)

Phone: (406) 207-7955

Department of Ecology, Evolution, and Behavior

University of Minnesota

1987 Upper Buford Circle 55108, Saint Paul, Minnesota, USA

Funding:

This work was supported by a National Science Foundation grant to AS (BCS 1461576). GS received funding from the NSF Experimental Program to Stimulate Competitive Research (EPSCoR) Track-1 EPS-1101342 (INSTEP 3).

Abstract

Predicted increases in forest drought mortality highlight the need for predictors of incipient drought-induced mortality (DIM) risk that enable proactive large-scale management. Such predictors should be consistent across plants with varying morphology and physiology. Because of their integrative nature, indicators of water status are promising candidates for real time monitoring of DIM, particularly if they standardize morphological differences among plants. We assessed the extent to which differences in morphology and physiology between *Pinus ponderosa* populations influence time to mortality and the predictive power of key indicators of DIM risk. Time to incipient mortality differed between populations but occurred at the same relative water content (RWC) and water potential (WP). RWC and WP were more accurate predictors of drought mortality risk than other physiological indicators, including non-structural carbohydrate (NSC)

content and percent loss of conductivity (PLC). These results highlight that variables related to water status capture critical thresholds during DIM and the associated dehydration processes. Both WP and RWC are promising candidates for large-scale assessments of DIM risk. RWC is of special interest because it allows comparisons across different morphologies and can be remotely sensed. Our results offer promise for real time landscape-level monitoring of DIM and its global impacts.

Keywords: Drought, hydraulic failure, intraspecific variation, morphology, mortality, physiology, non-structural carbohydrates, seedlings, water content, water potential.

Acknowledgements

The authors thank L. Fishman for providing invaluable greenhouse space and constant insights and P. Demaree for his help collecting data. This project was part of a larger collaboration with S. Dobrowski and M. Maneta, who provided valuable input. A. Woods, B. Roskilly, R. Montgomery, S. Kothari, A. Castillo Castillo, R. Partelli, and L. Schroeder provided comments in early versions of this manuscript.

Introduction

Drought-induced forest mortality (DIM) is expected to increase across many regions with climate change (Dai 2013; Trenberth *et al.* 2014; Greenwood *et al.* 2017). Increases in DIM are expected to severely impact carbon cycles, species distributions, the economy, and global climate (Allen, Breshears & McDowell 2015). To anticipate DIM, indicators must allow real time monitoring of DIM risk. At the landscape level, such indicators must accurately predict DIM risk independently of physiological and morphological variation across and within species causing plants to differ in performance under drought (Cregg 1994). Much of the emphasis on plant drought responses and vulnerability to drought mortality has been at the species level (Bartlett, Scoffoni & Sack 2012; Choat *et al.* 2012). In contrast, variation within species, particularly species with wide distribution ranges and substantial morphological and physiological variation, is often overlooked despite the influence of such variation on drought performance (Cregg 1994; Tognetti, Michelozzi & Giovannelli 1997; Sergent, Bréda, Sanchez, Bastein & Rozenberg 2014; Garcia-Forner, Sala, Biel, Savé & Martínez-Vilalta 2016; Umaña & Swenson 2019). Hence, accurate, real time monitoring of DIM risk at large scales requires indicators of DIM risk that are robust and consistent regardless of variation in plant morphology and physiology. Additionally, for proactive management purposes, DIM indicators are most useful when, in addition to capturing the degree of DIM risk at a given level of drought, they can also distinguish the threshold at which a healthy population (no risk) becomes at risk of DIM (incipient mortality threshold) (Martinez-Vilalta, Anderegg, Sapes & Sala 2019; Sapes *et al.* 2019). Thus, the first step towards accurate, real-time, and large-scale monitoring of DIM risk is identifying indicators that show both consistent incipient mortality thresholds across populations as well as high predictive power of the actual DIM risk.

Mortality thresholds and the predictive power of DIM risk indicators may vary due to variation in morphology or physiology within and across species. For instance, wood density is positively related to resistance to cavitation (Hacke & Sperry 2001; Delzon, Douthe, Sala & Cochard 2010) and denser wood has been related to lower mortality rates (Greenwood *et al.* 2017). However, denser wood has also been shown to lead to higher mortality under drought (Hoffmann, Marchin, Abit & Lau 2011) highlighting that compensating factors such as deep roots (Padilla & Pugnaire 2016) or other strategies to avoid low water potential may offset the role of wood density. Similar patterns and offsetting mechanisms may occur within species if there is intraspecific variation in physiology and morphology. This example illustrates that robust

70 indicators of DIM risk should be insensitive to such variation so they can be used across a broad
71 range of plant types. Equally important is to identify indicators that can accurately assess DIM risk
72 from any organ available. For instance, leaf-based indicators will not be useful in plants that rely
73 on leaf shedding to survive under drought (Daubenmire 1972; Hastings, Oechel & Sionit 1989).
74 Indicators that can be measured in any organ are advantageous because they provide greater
75 measurement opportunities. However, to be useful for real-time, large-scale monitoring of DIM
76 risk, organ-specific indicators must have high predictive power and be consistent among each
77 other. Further, DIM risk indicators that integrate both morphological and physiological
78 adjustments are of critical interest because they are likely to show low variability in mortality
79 thresholds. Hence, assessing the relative consistency and predictive power of candidate predictors
80 of DIM risk across species, populations, and organs is important to identify useful large-scale
81 indicators of DIM risk.

82 Given that plants combine multiple strategies to maintain water balance (Mencuccini,
83 Minunno, Salmon, Martínez-Vilalta & Hölttä 2015), indicators of DIM that do not integrate their
84 combined effects may not show consistent incipient mortality thresholds and predictive power
85 among populations with varying strategies. Research on the mechanisms of DIM has identified
86 failure of water transport -measured as percent loss of conductivity (PLC)- as a common process
87 leading to DIM (Anderegg, Berry & Field 2012; Choat *et al.* 2012; Barigah *et al.* 2013; Hammond *et*
88 *al.* 2019). Non-structural carbohydrate (NSC) availability has also been shown to be important
89 (O'Brien, Leuzinger, Philipson, Tay & Hector 2014; Sapes *et al.* 2019), although the role is more
90 variable and still uncertain. While both water transport and NSC are needed to maintain water
91 balance and avoid DIM, other critical factors such as capacitance (Mcculloh, Johnson, Meinzer &
92 Woodruff 2014) and turgor (Guadagno *et al.* 2017, but see resurrection plants) are not integrated
93 in PLC or NSC measurements alone. Martínez-Vilalta et al. (2019) reasoned that water status
94 variables would be useful indicators of DIM risk because they directly reflect the plant water
95 balance and integrate the diverse processes and strategies -both morphological (Daubenmire
96 1972; Maherali & Pockman 2004; Matías, González-Díaz & Jump 2014) and physiological
97 (Subbarao, Nam, Chauhan & Johansen 2000; Meinzer *et al.* 2016)- that plants use to avoid lethal
98 dehydration. From all the water status variables, Martínez-Vilalta *et al.* (2019) highlighted water
99 potential and water content (including relative water content -RWC) as potential candidates for
100 assessment of DIM risk. However, they noted that water potential varies enormously across
101 species (Bartlett *et al.* 2012; Choat *et al.* 2012) thus making predictions species-specific (Venturas

et al. 2018; Simeone *et al.* 2019) and suggested that RWC would be less variable. Consistent with the argument in Martínez-Vilalta *et al.* (2019), Sapes *et al.* 2019 showed that plant volumetric water content integrates the effects of PLC and NSC depletion - critical physiological processes leading to dehydration and DIM- and predicts DIM risk with high accuracy.

Indicators of plant water content are likely to display consistent incipient mortality thresholds and these thresholds are likely detectable via remote sensing. To remain alive and functional, cells must avoid permanent turgor loss which leads to cellular damage and plant death (Guadagno *et al.* 2017). Because cell turgor requires maintaining cell water volume above certain thresholds, plants are likely to show increasing mortality risk once RWC reaches the turgor loss point. RWC is of special interest because it reflects the amount of water present in a plant, organ, or tissue relative to the maximum it can hold (Barrs & Weatherley 1962; see below). Capturing the true maximum water content of plants can be sometimes as methodologically challenging as finding the true maximum hydraulic conductivity, the true minimum water potential in the field, or the true NSC concentrations of a species (Sanders & Arndt 2012; Quentin *et al.* 2015; Fontes & Cavender-Bares 2019). However, when maximum water content is correctly captured, RWC thresholds will likely be more consistent among individuals or species because RWC accounts for potential differences in maximum water content due to varying anatomy. Additionally, RWC reflects the integrated effects of the physiological and morphological adjustments that plants undergo to maintain water balance and prevent turgor loss, and it is likely to be more consistent among populations and species than other less integrative indicators. Accordingly, Bartlett *et al.* 2012 showed that turgor loss occurs at similar RWC (but different water potential) across species from different biomes, which inherently vary in morphology and physiology. The common RWC values at turgor loss across species could indicate a common degree of maximum dehydration that most woody plants can withstand prior to risking death. Lastly -and unlike PLC and NSC-, a clear advantage of plant water content is that it can be estimated from organs to ecosystems via remote sensing (Ullah, Skidmore, Naeem & Schlerf 2012; Wang & Li 2012; Mirzaie *et al.* 2014; Rao, Anderegg, Sala, Martínez-Vilalta & Konings 2019; Marusig *et al.* 2020). Several remote sensing studies have observed declines in canopy water content followed by increased drought mortality (Saatchi *et al.* 2013; Asner *et al.* 2015). The potential for consistency and the fact that water content can be remotely sensed, make RWC a great candidate for large-scale assessments of DIM risk.

We performed a greenhouse drought experiment based on the point of no return (i.e., no recovery after re-watering) with one-year-old ponderosa pine (*Pinus ponderosa* Douglas ex C. Lawson) seedlings to assess the extent to which morphological and physiological variation translate into differences in incipient population-level mortality thresholds and predictive power of four potential indicators of DIM risk: PLC, NSC, water potential, and RWC. We used a common garden approach with two genetically differentiated seedling provenances (North Plateau and Northern Rocky Mountain) (Potter, Hipkins, Mahalovich & Means 2013) known to differ in responses to drought (Cregg 1994). We focused on variability among populations and organs. Specifically, we withheld water and asked 1) do populations differ in mortality rates over time?, 2) if so, what physiological and morphological differences contribute to differences in mortality rates?, and 3) do water status variables such as water potential and RWC show higher predictive power and more consistent incipient mortality thresholds across populations and organs relative to other indicators of DIM such as PLC and NSC?

Materials and Methods

Study Design

We performed a greenhouse drought experiment at the University of Montana greenhouse facilities with one-year old ponderosa pine (*Pinus ponderosa* Douglas ex. C. Lawson) seedlings from two genetically differentiated populations known as the North Plateau race (NP) (42.6 N 122.8 W) and the Northern Rocky Mountain race (RM) (45.9 N 104.5 W) (Potter *et al.* 2013). Ponderosa pine is one of the most widely distributed species in North America and has been extensively used as a representative gymnosperm in ecological, physiological, and forestry studies. We chose one-year old seedlings because of their biological relevance for regeneration of lower tree-line forests which is constrained by dry conditions (Simeone *et al.* 2019). On May 25th 2016 we planted 250 individuals from seed provided by the USDA Forest Service in 7.62 cm diameter x 43 cm tall pots using a homogeneous soil mixture consisting of 3:1:1 sand, peat moss, and top soil. Seeds started to germinate by June 2nd and seedlings were grown at soil field capacity until they were big enough to be measured (ca. 6 cm height and 2.5 cm basal diameter), which corresponded to February 24th 2017. Soil field capacity corresponded to soil volumetric water content values (VWC_s) of ca. 20%. We monitored changes in VWC_s using Meter 5TE sensors placed 10 cm above the bottom of the pots in five representative seedlings of each population. Sensors were inserted through a hole previously drilled in the side of the pots to minimize disturbance of

soil structure and root system damage, which started to reach the bottom of the pot by the end of the experiment.

From February 24th 2017 to May 11th, seedlings underwent three drought pre-conditioning cycles to simulate early summer conditions. During the first two cycles, we dried pots down to 50% of their field capacity (VWC_s = 10%) after which we watered again to field capacity. On the last cycle, pots were dried down to 25% of their field capacity (VWC_s = 5%), which corresponds to a soil water potential of -0.7 MPa based on an empirical soil characteristic curve (see below), and then watered again to field capacity. This drought preconditioning provided a more realistic response to experimental severe drought since plants were able to acclimate to increasing drought as it tends to occur in natural conditions. After the drought-preconditioning, water was withheld (final drought) in all seedlings except a control group which was kept at field capacity. Based on a preliminary drought experiment to assess symptoms of mortality as a function of soil drought and to optimize sampling times and sample size, we started measurements 29 days after the start of the drought treatment.

Sampling procedure

We assessed the degree of drought (i.e. soil water potential), seedling physiology, and mortality risk on six weekly samplings starting on day 29 of the drought treatment. At each sampling, we measured midday VWC_s in five randomly chosen seedlings from each population and we used VWC_s to estimate soil water potential based on soil water-retention curves specific for our soil type as in Sapes *et al.* (2019). VWC_s sensors were installed 24h prior to measurements to reach equilibrium with soil conditions. We used the same seedlings where VWC_s was measured to assess mid-day leaf and stem water potential. Leaf water potential was measured in a single needle bundle using a pressure chamber (PMS Instrument Company, Corvallis, OR) following methods in (Kaufmann 1968). Stem water potentials were estimated by equilibrating the water potential of a needle bundle with the stem following methods from Begg & Turner (1970) and measuring the equilibrated bundle with the pressure chamber. We also took midday measurements of stomatal conductance and dark respiration rates per unit leaf area in each seedling using a Licor 6400 XT equipped with a 6400 RED LED chamber. CO_2, flow, temperature, and relative humidity were set constant at 400 µmol s^{-1}, 100 mol s^{-1}, 25 ºC, and 50%, respectively. Light conditions were set at 1,000 µmol quanta m^{-2} s^{-1} for stomatal conductance measurements and the light was turned off to measure dark respiration. We scaled up stomatal conductance to

195 the canopy level (i.e., canopy conductance) by multiplying it by canopy leaf area (see methods S1).
196 After this, seedlings were immediately harvested, morphology was measured (see methods S1),
197 and seedlings were transferred to zip-lock bags with a moist paper towel in a cooler to prevent
198 water loss (Garcia-Forner *et al.* 2016). Seedlings were then transported to the laboratory within
199 two hours for hydraulic and water content measurements (see below). Because we could not
200 assess mortality risk in plants that were harvested, we randomly chose a second independent
201 subset of seedlings at each sampling event to assess mortality risk at any given point during the
202 drought (see below).

203 **Mortality assessment**

204 We estimated the probability of mortality at the population level over time as in Sapes *et*
205 *al.* (2019). In our study, population-level mortality is defined as the proportion of individuals from
206 each population sampled at a given time that end up dying. At each sampling event, five groups of
207 six seedlings (total of 30) were randomly chosen, classified as dead or alive, re-watered to field
208 capacity, and kept well-watered until September 22nd to confirm mortality assessments. This
209 method ensures accurate classification of both live and dead plants at every sampling event. Then,
210 we classified seedlings as dead, only if their canopy and phloem were completely brown and dry
211 after a month of re-watering and no subsequent buds appeared (Cregg 1994). We calculated
212 mortality as the proportion of dead seedlings (out of 30) at a given sampling time. Note that in our
213 design, physiological measurements during drought were done in individual plants, while mortality
214 measurements were conducted at the population level. Thus, one value of probability of mortality
215 is always associated to five individual values that reflect the variation in physiological status across
216 the population.

217 **Relative Water Content**

218 Upon arrival to the laboratory, we separated roots, stems, and needles of each seedling to
219 measure their relative water content (RWC) based on fresh, saturated, and dry weights as: ((Fresh
220 weight-Dry weight)/Saturated weight-Dry weight)*100 (Barrs & Weatherley 1962). Saturated
221 weight was obtained by rehydrating needles for 5 hours in the dark at low temperatures (3 ºC).
222 Low temperatures prevent oversaturation artifacts that arise due to artificially low osmotic
223 potential resulting from catabolic conversion of starch into sugars (Boyer, James, Munns, Condon
224 & Passioura 2008). We calculated whole plant RWC weighed by organ biomass fraction
225 (proportion of each organ dry mass fraction multiplied by their respective RWC). Population-level

226 pressure-volume curves were also built using midday leaf water potentials and the corresponding
227 leaf RWC of each individual as in Tyree *et al.* (2002) and leaf RWC at turgor loss and water
228 potential at turgor loss were extracted for each population.

229 **Stem and Root Hydraulics**

230 Native hydraulic conductivity

231 We measured stem hydraulic conductivity and root hydraulic conductance using the
232 gravimetric method (Sperry, Donnelly & Tyree 1988) immediately after organ fresh weight
233 measurements. We used the same apparatus and methods described in Sapes *et al.* (2019). Stem
234 segments previously used for RWC measurements were immersed in deionized water for 20
235 minutes to relax xylem tensions that could artificially alter conductivity values (Trifilo, Barbera,
236 Raimondo, Nardini & Gullo 2014). After relaxation, stems were relocated to the hydraulic
237 apparatus and each end was recut twice at a distance of 1 mm from the tips each time (total of 2
238 mm per side) to remove any potential emboli resulting from previous cuts, transport, and
239 relocation (Torres-Ruiz *et al.* 2015). Stems were then connected to the hydraulic apparatus while
240 under water, with their terminal ends facing downstream flow. The stems were then raised out of
241 the water and the connections were checked to ensure that there were no leaks. A solution of
242 water with 10 mM KCl degassed at 3 kPa for at least 8 hours was used for all hydraulic
243 measurements (Espino & Schenk 2011).

244 First, initial background flow was measured to account for the flow existing under no
245 pressure, which can vary depending on the degree of dryness of the measured tissue (Hacke *et al.*
246 2000; Torres-Ruiz, Sperry & Fernández 2012; Blackman *et al.* 2016). Second, a small pressure
247 gradient of 5-8 kPa was applied to run water through the stem and pressurized flow was
248 measured. Lastly, final background flow was measured, initial and final background flows were
249 averaged, and flow was calculated as the difference between pressurized flow and average
250 background flow. Native specific hydraulic conductivity (K) was estimated in stems as the flow
251 divided by the pressure gradient used and standardized by xylem area and length. In root systems,
252 flow was measured as above and whole root native hydraulic conductance (k) was estimated as
253 the flow divided by the pressure gradient used and standardized by xylem area at the root collar.

254 Percent loss hydraulic conductivity

255 Maximum stem hydraulic conductivity (Kmax) and root hydraulic conductance (kmax)
256 were estimated at the population level as the average stem K and root k of the pre-conditioned
257 control measured at day 0 since the onset of the drought. Such a population approach was
258 necessary because 1) destructive measurements in these small seedlings prevented successive
259 measurements of K and water potential on the same individuals, and 2) flushing and vacuum
260 infiltration techniques to obtain Kmax from embolized tissues can generate artifacts and
261 overestimate Kmax (Cochard *et al.* 2013). Percent loss of stem conductivity and root conductance
262 were estimated for each measured seedling as 100*(Kmax-K)/Kmax and 100*(kmax-k)/kmax,
263 respectively. Note that negative PLC values may occur when K or k in a given sample is larger than
264 Kmax estimated as the average K or k of controls. We calculated whole-plant PLC weighted by
265 organ fraction. Root and stem PLC can be averaged together because they are unit-less indexes
266 that represent the relative loss of water transport capacity of their respective organs. Because we
267 did not measure PLC in needles, whole-plant PLC represents the overall hydraulic integrity of the
268 stem and root systems. We excluded negative PLC values resulting from uncertainty around
269 population level estimates of Kmax (Sapes *et al.* 2019). We ensured that exclusion of data was
270 homogeneous across populations and sampling times (Table S1) to avoid influencing comparisons
271 between populations.

272 **Non-structural Carbohydrates**

273 After hydraulic measurements, non-structural carbohydrates were analyzed in all tissue
274 types (needles, stems, and roots) collected at harvest. A sample of each tissue was microwaved for
275 180 seconds at 900 Watts in three cycles of 60 seconds to stop metabolic consumption of NSC
276 pools, and oven-dried at 70 ^{o}C. Samples were dried to a constant mass and finely ground into a
277 homogenous powder. Approximately 11 mg of needle tissue and 13 mg of stem or root tissue
278 were used to analyze NSC dry mass content following the procedures and enzymatic digestion
279 method from Hoch, Popp & Körner (2002) and Galiano, Martínez-Vilalta, Sabaté & Lloret (2012).
280 NSC, starch, sucrose, and glucose + fructose tissue concentrations were then multiplied by their
281 respective tissue fraction (the dry mass of a tissue relative to whole-plant dry mass) to obtain
282 whole-plant concentrations. Whole-plant dry mass for each seedling was calculated by combining
283 the dry mass of all samples and the remaining biomass. For the sake of space, these methods are
284 described in detail in Methods S1.

285 **Statistical analyses**

286 We assessed differences in morphology between populations across the full set of
287 measurements using two-tailed Student's t-test for independent samples. Canopy leaf area, root
288 to shoot ratios, organ biomass, whole-plant biomass, and plant length were used as dependent
289 variables and population was the categorical variable in all tests. Differences in maximum stem
290 hydraulic conductivity between populations (based on K of control plants) were also tested using
291 the same approach. Variables were transformed to achieve normality and homogeneity of
292 variances when needed. We also assessed potential differences in hydraulic conductivity due to
293 plant length given that trees are known to increase hydraulic conductivity at the base of the stem
294 as they grow tall to minimize the resistance of the hydraulic pathway (Olson *et al.* 2018).
295 Differences in hydraulic conductivity as a function of plant length were assessed in two linear
296 models with stem hydraulic conductivity and root hydraulic conductance as response variables,
297 respectively, and plant length, population, and their interaction as predictors. Response variables
298 were log-transformed to meet model assumptions.

299 We assessed differences in response to drought over time between populations by
300 splitting the drought into early drought (days 0 and 29) and late drought (days 29 to 72). This was
301 necessary because physiological measurements were not taken between days 0 and 29 to
302 maximize sampling after the onset of mortality. Thus, analyses from day 29 to 72 reflect responses
303 close to and after the onset of mortality in the population (when a few individuals start to die) and
304 characterize the processes that either prevent or ultimately lead to death. Early differences in
305 response to drought between populations were tested using two-tailed Student's t-test for
306 independent samples at day 0 and 29. T-tests were used instead of regressions because data
307 included only two days. Soil and plant water potentials, canopy conductance, PLC, NSC, and RWC
308 across organs at day 0 and 29 were used as dependent variables while population was the
309 categorical variable in all tests. Contrasts from day 0 to 29 provide information of whether
310 observed differences after the onset of mortality originated during early stages prior to mortality.

311 Differences in response to drought between populations after day 29 were assessed using
312 three sets of regression models with data until day 72. Response variables were i) soil, leaf, or
313 stem water potential to represent the degree of drought intensity; ii) whole-plant PLC, whole-
314 plant NSC, or whole-plant RWC to represent loss of hydraulic function, NSC depletion, and degree
315 of dehydration; and iii) population-level mortality to represent the probability of DIM. All models
316 had days since the 29th day of drought, population, and the interaction of both factors as the

317 predictor variables. Generalized linear models (Mardia, Kent & Bibby 1979) with binomial
318 distribution and logit link were used for models including probability of mortality. Linear models
319 were used for all other cases as the response variables showed a linear response with time or
320 could be transformed to meet assumptions of linearity.

321 We took a residuals approach to explore whether differences in dehydration rates leading
322 to death between populations were driven by morphology, physiology, or both. First, we extracted
323 the residuals from a model with RWC as the response variable and days since the onset of drought
324 as the predictor. In this initial model, the residuals reflect variation in dehydration rates across
325 populations not explained by time under drought due to individual variation in morphological and
326 physiological characteristics. We chose RWC as our response variable because dehydration is the
327 main process leading to DIM (Tyree *et al.* 2003; Martinez-Vilalta *et al.* 2019; Sapes *et al.* 2019) and
328 integrates the physiological (e.g. low stomatal conductance, maintenance of hydraulic function,
329 NSC depletion) and morphological (e.g. low canopy area, high root to shoot ratios, reduced
330 growth) responses to prevent dehydration leading to DIM risk. Then, we built a second model for
331 morphology with the residual variation of the first model as the response variable and population,
332 root to shoot ratios, whole-plant biomass and all the interactions as predictive variables. In this
333 model, significant effects of morphological variables indicate that, regardless of population of
334 origin, morphology explains variation in dehydration rates that is not explained by time under
335 drought. Significant interactions between a given morphological variable and population indicate
336 that the effects of morphology are population-specific. Thus, a significant effect of population
337 alone or as part of an interaction indicates that morphological differences alone are not able to
338 explain all the variation in dehydration rates between populations. We followed the same
339 approach to test the influence of physiology in a third model where we used physiological
340 variables (stomatal conductance, dark respiration, whole-plant PLC, and whole-plant NSC) instead
341 of morphological variables as predictive variables. Morphological variables were log-transformed
342 to meet model assumptions. Other physiological (e.g., soil and plant water potential) or
343 morphological (e.g., plant length and canopy area) variables were excluded from these models
344 because they were highly correlated with the selected predictor variables. Using whole-plant
345 variables also allowed us to account for potential organ-specific effects without increasing the
346 number of predictors or violating assumptions of co-linearity.

347 We used logistic regressions (Walker & Duncan 1967) to assess the predictive power and
348 consistency of each mortality predictor and search for potential thresholds indicative of incipient
349 mortality risk. For each organ within a population, logistic models included probability of mortality
350 as the response variable, and RWC, water potential, PLC, or NSC as predictors. Probability of
351 mortality was expressed as a decimal fraction following requirements of models with binomial
352 distributions. Predictive power was estimated as the proportion of variance explained (VE) by each
353 model (i.e., [1- residual variance/null variance] x 100) (Guisan & Zimmermann 2000). In logistic
354 models, VE is often discouraged because it tends to underestimate predictive power due to the
355 lack of values between 0 and 1 in the response variable. However, population-level mortality does
356 contain intermediate values between 0 and 1 thus overcoming this issue. We assessed the
357 consistency of mortality curves within each predictor by testing differences in slopes and
358 intercepts of mortality relationships across populations and organs using another set of logistic
359 models containing the interaction between a given predictor, population, and organ. In these
360 models, non-significant interactions were not removed because our hypothesis explicitly tested
361 the interaction between population, organ, and each predictor.

362 We identify incipient mortality thresholds in logistic regression models as the value of the
363 physiological predictor beyond which mortality risk suddenly increases. To identify incipient
364 threshold values in each mortality curve, we used a mathematical approach similar to Gregorczyk
365 (1998) and Mischan, Pinho & Carvalho (2011) based on the third derivative of the logistic
366 regression function (Fig. 1, see Methods S2). The third derivative describes changes in the
367 acceleration of mortality rates as physiological status (the predictor variable) declines. It detects
368 incipient mortality thresholds as a peak - maximum or minimum depending on the nature of the
369 physiological predictor - near the wet end of the range of physiological values (Fig. 1), indicating a
370 sudden change of acceleration of mortality rates (i.e., a threshold). We extracted threshold values
371 for all mortality curves (Methods S3) and compared their degree of incipiency (probability of
372 mortality at the threshold) and their consistency among physiological predictors. To assess
373 consistency among organs and populations within a given predictor, we constructed a unitless
374 index that considers the average value of the physiological predictor at the mortality threshold
375 across all mortality curves and describes how the threshold of each curve deviates from the
376 average value (Methods S2). We compared threshold incipiency, threshold consistency, and
377 variance explained among predictors using ANOVA and Tukey Honest Significant Difference tests.
378 All analyses were performed using R version 3.6.3 (R Core Team 2020).

Results

North Plateau (NP) seedlings were longer (from root tip to stem tip) ($t = 2.51$, $p = 0.014$; Fig. 2a) and had greater whole-plant biomass ($t = 3.58$, $p < 0.001$; Fig. 2b) than Northern Rocky Mountain (RM) seedlings (all dates combined). These differences were due to greater stem ($t = 5.04$, $p < 0.001$; Fig. S1a) and root biomass ($t = 5.43$, $p < 0.001$; Fig. S1b) in NP seedlings. Differences in biomass allocation translated to greater root to shoot ratios in NP seedlings ($t = 4.83$, $p < 0.001$; Fig. 2c). Differences in plant length between populations were associated with greater hydraulic conductivity in NP seedlings (stem: $R^2_{adj} = 0.18$, plant length: $p < 0.001$, population: $p = 0.077$; roots: $R^2_{adj} = 0.08$, plant length: $p = 0.003$, population: $p = 0.047$; Table S2). Accordingly, NP seedlings also had greater stem maximum hydraulic conductivity ($t = 1.94$, $p = 0.059$; Fig. S1c).

Up to day 29, the probability of mortality was zero in both populations (Fig. 3e). Mortality risk started to increase above zero by days 29 and 42 in NP and RM populations, respectively (Fig. 3d). After the onset of mortality in each population, mortality probabilities increased at the same rate in both populations.

At the beginning of the experiment (day 0), populations only showed physiological differences in dark respiration, with RM seedlings respiring more than NP seedlings ($t = 2.25$, $p = 0.04$; data not shown). These differences disappeared by day 29 of drought. In contrast, at day 29, NP seedlings had lower whole-plant RWC ($t = -4.57$, $p = 0.002$), which was driven by lower stem and root RWC (stem: $t = -4.70$, $p = 0.003$; roots: $t = -2.25$ $p = 0.056$). These results indicate that NP seedlings experienced greater dehydration rates during the early stages of the drought. Soil, stem, and leaf water potentials were also consistently lower in NP seedlings by day 29, but differences were not statistically significant.

At late stages of drought (day 29 to 72), the soil water potentials of the two populations clearly diverged and continued to decrease at similar rates ($R^2_{adj} = 0.30$, days: $p < 0.001$; population: $p = 0.029$; Fig. 3a, Table S3). The same pattern was observed for leaf and stem water potentials (needles: $R^2_{adj} = 0.77$, days: $p < 0.001$, population: $p = 0.031$; stems: $R^2_{adj} = 0.83$, days: $p < 0.001$, population: $p = 0.065$; Fig. 3a, Table S3). Declines in water potential were accompanied by increases in PLC in both populations, but PLC in NP seedlings increased faster than in RM seedlings ($R^2_{adj} = 0.57$, days: $p < 0.001$, days x population: $p < 0.022$; Fig. 3b, Table S3). This pattern was driven by higher PLC rates in roots ($R^2_{adj} = 0.27$, days: $p < 0.001$, population: $p = 0.044$, days x

410 population: $p < 0.011$; Fig. 3b, Table S3), which were explained by higher root to shoot ratios in NP
411 seedlings ($R^2_{adj} = 0.60$, days: $p < 0.001$, root shoot ratio: $p = 0.035$, days x population: $p = 0.018$;
412 Fig. S2, Table S3). By day 29, NP seedlings also had higher stem and root NSC (relative to controls)
413 than RM seedlings. However, they also consumed NSC in their roots at a faster rate than RM
414 seedlings throughout the drought (plant: $R^2_{adj} = 0.57$, days: $p < 0.001$, population: $p < 0.001$;
415 needles: $R^2_{adj} = 0.16$, days: $p < 0.001$; stems: $R^2_{adj} = 0.38$, days: $p < 0.001$, population: $p < 0.001$;
416 roots: $R^2_{adj} = 0.16$, days: $p < 0.001$, days x population: $p = 0.014$; Fig. 3c, Table S3). Finally, NP
417 seedlings lost RWC in needles at faster rates than RM seedlings ($R^2_{adj} = 0.78$, days: $p < 0.001$, days x
418 population: $p = 0.030$; Fig. 3d, Table S3). In turn, differences in dehydration rates in needles led to
419 marginally lower canopy conductance rates in NP seedlings ($R^2_{adj} = 0.03$, days: $p = 0.071$,
420 population: $p = 0.055$, days x population: $p = 0.079$; Table S3). While leaves of NP seedlings
421 dehydrated faster (i.e., different slopes between populations), this trend was not observed at the
422 whole plant level because needles were a very small fraction of the biomass and therefore
423 contribute little to the whole-plant water content. However, whole-plant RWC still differed
424 between populations (i.e. different intercepts between populations) ($R^2_{adj} = 0.71$, days: $p < 0.001$,
425 population: $p < 0.001$; Fig. 3d, Table S3) as observed during early drought stages (day 29). As a
426 result, NP seedlings started dying more than two weeks earlier but both populations showed
427 similar rates of mortality once mortality started (days: $p < 0.001$; population: $p = 0.024$; Fig. 3e,
428 Table S3).

429 Residual analyses allowed us to determine whether differences in dehydration rates
430 between populations were explained by differences in morphology, physiology, or both. Variation
431 in dehydration rates unrelated to time since drought was partially attributed to physiology but
432 population was still significant ($R^2_{adj} = 0.46$, population: $p = 0.05$, respiration: $p = 0.005$, population
433 x stomatal conductance: $p = 0.002$, respiration x whole-plant PLC: $p = 0.001$, population x stomatal
434 conductance x whole-plant PLC: $p < 0.001$). This indicates that physiological differences alone
435 cannot fully explain the differences in dehydration rates observed between populations. On the
436 other hand, population was not significant when the remaining variation was attributed to
437 morphology ($R^2_{adj} = 0.32$, log(root to shoot ratio): $p = 0.002$, log(plant biomass): $p = 0.013$). This
438 indicates that morphological differences in root to shoot ratios and plant size alone can explain the
439 differences in dehydration rates observed between populations. That is, morphological variables
440 absorb the variation otherwise explained by the categorical variable 'population' thus making it
441 not significant.

The ability of PLC, NSC, water potential, and RWC to predict mortality varied among populations and organs, both in terms of predictive power and degree of significance (Figs. 4c, 5; Table S5). Water status variables (RWC and water potential) had comparably high predictive power (RWC: p-value$_{Range}$ = <0.001 - 0.002, VE$_{Average}$ = 76.35%, VE$_{Range}$: 54%-95%; water potential: p-value$_{Range}$ = <0.001 - 0.01, VE$_{Average}$ = 74.42%, VE$_{Range}$: 46%-93%). Additionally, both variables showed similar relationships with DIM risk across organs and populations as supported by the lack of significant differences in intercepts and slopes (Fig. 5a-b, Table S6). The predictive power of NSC relative to control and the degree of significance were lower than for water status variables and more variable across organs and populations (p-value$_{Range}$ = 0.001 - 0.056, VE$_{Average}$ = 41%, VE$_{Range}$: 15%-63%; Fig. 4c). PLC had similar predictive power than NSC (p-value$_{Range}$ = <0.001 - 0.564, VE$_{Average}$ = 42.78%; Fig. 4c) but predictive power varied the most among populations and organs (VE$_{Range}$: 1%-76%; Fig. 4c & 5b, Table S5). This result, however, should be interpreted with caution due to greater uncertainty in hydraulic conductivity measurements in RM seedlings because of their small size and low flow rates.

Logistic regressions identified mortality thresholds in all variables (Fig. 5). For RWC and water potential, incipient mortality thresholds were apparent in all organs measured and in the two populations (Fig. 5a-b). RWC showed the greatest degree of incipiency in mortality thresholds followed by water potential and PLC and lastly by NSC (Fig. 4a). Importantly, both RWC and water potential showed mortality thresholds close to the values corresponding to leaf turgor loss (Fig. 5a-b, vertical lines). In contrast, thresholds for NSC and PLC were not always apparent and/or less consistent across populations (Fig. 5c-d & Fig. 4b): NSC thresholds were apparent in all organs in the RM population only, while PLC thresholds were only apparent in the NP population (Fig. 5c-d).

Discussion

It has long been known that individuals of the same species can show morphological and physiological differences across the landscape. Our results in a ponderosa pine common garden experiment suggest that such differences can affect the predictive power and mortality thresholds of DIM risk indicators. Hence, it is critical to find which DIM indicators are the least sensitive to individual variation across the landscape. Our results show that DIM indicators related to plant water status show high and least variable predictive power across populations and organs. Among these, RWC standardizes morphological differences among individuals, likely explaining why it provides consistent incipient mortality thresholds among populations and organs. Because of its

473 consistency and high predictive power -and because it can be estimated via remote sensing-, RWC
474 emerges as a promising indicator to monitor real time DIM risk across the landscape.

475 Morphological and physiological differences between populations explained
476 dehydration rates and time to death. Critically, morphology and physiology played in concert
477 under drought stress. All pots were similar in size and contained the same soil mixture thus
478 holding similar amounts of water at the start of the drought. Hence, differences in dehydration
479 rates between populations can be attributed to differences in water consumption during the
480 drought. NP seedlings grew taller and bigger than RM seedlings and had built much greater root
481 biomass prior to the onset of drought resulting in greater root:shoot ratios (Fig. 2a-c). NP seedlings
482 also grew longer from the tip of roots to the tip of shoots prior to the drought (Fig. 2a), which
483 increased the resistance to water flow through the plant due to a longer hydraulic pathway. To
484 compensate for this increase, NP seedlings -like other plants- developed greater maximum stem
485 hydraulic conductivity (Fig. S1, Olson *et al.* 2018), an allometric pattern caused by downwards-
486 widening of stem xylem conduits and that is likely to extend into the roots (Carrer, Von Arx,
487 Castagneri & Petit 2014). Increased stem hydraulic conductivity along with greater root biomass
488 allowed NP seedlings to transport more water (i.e., greater hydraulic efficiency) and maintain
489 growth rates under well-watered conditions. However, greater hydraulic efficiency and plant size
490 came at the cost of greater soil water consumption (Fig. 3a), lower soil water potential, greater
491 cavitation rates (Fig. 3b, Fig. S2) and earlier death during drought (Fig. 3e). The smaller size and
492 lower hydraulic efficiency of RM seedlings was an advantage under drought and led to slower
493 dehydration and mortality rates (Fig. 3d-e). RWC captured all this morphological and physiological
494 variation and its consequences during the dehydration process: NP seedlings dehydrated faster
495 than RM seedlings and reached lethal thresholds earlier, thus, condensing the RWC-mortality
496 functions of both populations into a smaller space (Fig. 5a).

497 Because DIM is a gradual dehydration process, variables directly reflecting plant water
498 status are good candidates for indicators of DIM risk. The challenge lies in identifying which water-
499 status variables may best indicate how much dehydration leads to death for any given plant
500 population or species at any given location. Large scale monitoring requires variables applicable at
501 different scales and that are reasonably consistent across plant organs, populations, and species.
502 Earlier, we made the argument that RWC could be a promising candidate because of several
503 reasons. RWC reflects the interactions between water transport and carbohydrate availability that

504 determine plant water balance (uptake and loss) (Sapes *et al.* 2019) and the combined effects of
505 both morphology and physiology on dehydration time (Table S4) (Martinez-Vilalta *et al.* 2019).
506 RWC, like water potential, can also detect the transition to turgor loss (using RWC_{TLP}), which has
507 been associated to cellular and organ death under drought (Guadagno *et al.* 2017). Our results
508 across two differentiated ponderosa pine populations partially support our prediction that RWC
509 would be the most suitable predictor of DIM risk for large scale assessments in several ways. First,
510 RWC accurately predicted DIM risk across populations and organs despite the differences in
511 physiology and morphology and the differences in time to death. Second, both populations died at
512 the same RWC, and incipient mortality thresholds of RWC were also relatively consistent across
513 organs. Finally, incipient mortality thresholds of RWC coincided with the RWC_{TLP} and DIM risk
514 increased with further declines in RWC, consistent with the increase in cellular damage that
515 follows turgor loss (Guadagno *et al.* 2017). However, in contrast to our prediction, water potential
516 was also a particularly good predictor of DIM risk, was quite consistent across organs and
517 populations and showed consistent -but slightly less incipient- mortality thresholds close to turgor
518 loss point. Therefore, in ponderosa pine, both RWC and water potential are good indicators of DIM
519 risk. In contrast, neither NSC nor PLC were as good candidates (but see below).

520 Plant water potential may be a good indicator of real-time DIM risk within species but may
521 pose challenges in landscape-level assessments when multiple species are present. In our
522 experiment, plant water potential also showed high predictive power and consistent mortality
523 thresholds associated to turgor loss across both populations and organs. Low water potentials
524 cause embolism and stomatal closure which impair water transport and carbohydrate availability,
525 respectively (Tyree & Sperry 1989; Sevanto, McDowell, Dickman, Pangle & Pockman 2014;
526 Meinzer *et al.* 2016). Because both reduced water transport and carbohydrate availability are
527 involved in drought mortality (Mitchell *et al.* 2013), the predictive power of water potential is
528 likely high (Fig. 4b). Additionally, plant water potential also indicates wilting via the turgor loss
529 point (Ψ_{TLP}), thus explaining the observed degree of incipiency in mortality thresholds associated
530 with turgor loss (Fig. 5b). Indeed, these characteristics have made water potential one of the main
531 components of mechanistic DIM models (Sperry & Love 2015). The consistent water potential
532 thresholds and high predictive power we found in both populations suggest that -at least in
533 ponderosa pine- there is little variability in lethal water potentials among populations. These
534 results are consistent with relatively high vulnerability to embolism observed in ponderosa pine
535 (Piñol & Sala 2000; Martinez-Vilalta, Sala & Pinol 2004) and low intraspecific variability in

536 vulnerability to embolism (Maherali & DeLucia 2000; Stout & Sala 2003). However, plant water
537 potential is likely to show different incipient mortality thresholds across species given the large
538 variation in minimum water potentials (Choat *et al.* 2012) and in Ψ_{TLP} (Bartlett *et al.* 2012) across
539 species and biomes. Thus, despite its usefulness in mechanistic approaches, large-scale monitoring
540 of DIM based on remotely sensed water potential might only be applicable in monospecific or low
541 diversity forests in which pixels mostly contain a single species. In these instances, knowledge of
542 the Ψ_{TLP} of the species present may still be necessary to accurately predict thresholds leading to
543 DIM within the area of interest.

544 Neither NSC nor PLC were consistent predictors of DIM risk in our study. We expected PLC
545 to be a good predictor of DIM because it describes the capacity to transport water to living cells, a
546 critical function. Several studies have shown that conifers tend to experience mortality after
547 reaching PLC values above 50% (Brodribb and Cochard, 2009; but see Hammond et al., 2019). This
548 is particularly true in ponderosa pine where there is relatively little variation in vulnerability to
549 embolism among populations (Maherali & DeLucia 2000; Stout & Sala 2003). Consistently, DIM risk
550 increased in NP seedlings soon after reaching 50% PLC in stems and roots. However, PLC did not
551 predict DIM risk in RM seedlings due to very high variability. We believe that low flows in RM
552 seedlings caused by their small size likely generated uncertainty in PLC values, especially at later
553 stages of drought once seedlings embolized and reached flow rates close to the accuracy limit of
554 the sensor. Both the low intraspecific variability in vulnerability to embolism observed in Maherali
555 and DeLucia (2000) and the similar relationships between water potential (the causal agent of
556 emboli) and DIM risk found here support our supposition. Hence, the PLC results in RM seedlings
557 must be taken with caution. Even if PLC is a good predictor of DIM risk, it may still present
558 challenges similar to those for water potential (see above). NSC availability also showed variable
559 capacity to predict DIM risk and the lowest consistency in mortality thresholds. NSC availability has
560 been involved in drought mortality (Mitchell *et al.* 2013; Sevanto *et al.* 2014), but a recent
561 synthesis suggests mixed effects (Adams *et al.* 2017). Our results also showed some different
562 trends between the two populations. The greater root biomass in NP seedlings apparently
563 incurred greater NSC costs -as shown by greater root NSC consumption rates in NP seedlings (Fig.
564 3c)- and may have generated tradeoffs with other NSC-demanding functions such as
565 osmoregulation capacity (Sapes, Demaree, Lekberg & Sala 2020) and water retention, thus
566 contributing to faster dehydration. These tradeoffs could be less constraining in RM seedlings
567 because of their lower biomass and transpiration area. Hence, the lower NSC mortality thresholds

568 in RM seedlings (Fig. 5d). Interestingly, NSC availability showed increasing predictive power from
569 leaves to roots and was most predictive when considered at the whole plant level. Thus,
570 accurately predicting DIM risk based on NSC may require estimates of NSC content and biomass
571 across all organs.

572 Of the two indicators of water status that consistently predicted DIM between
573 populations, RWC has important benefits compared to water potential due to its relative nature.
574 Relative water content conveniently standardizes differences in maximum water content among
575 organs, individuals, and species, thus reducing the degree of variation in dehydration leading to
576 turgor loss point across plants (Bartlett *et al.* 2012). Accordingly, RWC showed consistent mortality
577 thresholds and relationships across organs and populations. Hence, RWC can be used to monitor
578 DIM risk in real time from any organ available such as stems or roots, which is of critical
579 importance given that drought-deciduous species shed leaves (Daubenmire 1972). In the case of
580 roots, we cannot estimate root water content remotely. However, and consistent with recent
581 studies (Nardini *et al.* 2020), the predictive power of root RWC highlights the importance of root
582 functioning and integrity during drought. Another benefit of RWC is that remote sensing estimates
583 of RWC could be similarly consistent across plants. Both RWC and water potential can be remotely
584 sensed (Cohen, Alchanatis, Meron, Saranga & Tsipris 2005; Zhang, Zhou, Gentine & Xiao 2019).
585 However, remote sensing estimates of plant water potential (i.e., xylem tension) are more likely to
586 reflect the diversity of morphology, physiology, and drought strategies (position within the iso-
587 anisohydric spectrum) within a pixel than to reflect DIM risk (Martinez-Vilalta *et al.* 2019). On the
588 other hand, RWC is directly related to plant water content and can be estimated across the
589 landscape using hyperspectral and thermal techniques (Ceccato, Flasse, Tarantola, Jacquemoud &
590 Grégoire 2001; Elsayed, Darwish, Elsayed & Darwish 2017; Konings *et al.* 2017). Remote sensing
591 estimates of plant water content -once standardized by the maximum values observed within a
592 pixel- are likely to show similar properties than RWC. While standardizing remote sensing
593 estimates of absolute plant water content is not a task lacking in challenges, recent work has
594 shown that this is indeed possible (Rao *et al.* 2019; Marusig *et al.* 2020). In summary, RWC stands
595 out as a good candidate for large-scale, real-time assessments of DIM risk.

596 Our study highlights a critical point: morphological and physiological differences among
597 populations can significantly influence mortality rates and the predictive capacity of DIM risk
598 indicators that are not associated with plant water pools. Hence, large-scale indicators of DIM risk

should be chosen based on the consistency and incipiency of their mortality thresholds and predictive power among populations and species. Doing so will ensure that such indicators can predict DIM risk across the landscape regardless of the existing intraspecific variation. Based on our results, RWC may achieve this because it integrates the physiological mechanisms of mortality under drought and standardizes morphological differences among individuals and populations. Future research should assess the consistency and incipiency of incipient mortality thresholds and the predictive power of RWC across species. Similarly, remote sensing estimates of RWC should be further developed (but see Rao *et al.* 2019; Marusig *et al.* 2020). Despite, the work that still lays ahead, we hope that our findings help increase the accuracy of current monitoring efforts and may open a path of research towards global scale assessments of DIM risk (Martinez-Vilalta *et al.* 2019).

Acknowledgements

This work was supported by a National Science Foundation grant to AS (BCS 1461576). GS received funding from the NSF Experimental Program to Stimulate Competitive Research (EPSCoR) Track-1 EPS-1101342 (INSTEP 3). The authors thank L. Fishman for providing invaluable greenhouse space and constant insights, P. Demaree for his help collecting data and S. Dobrowski, A. Woods, B. Roskilly, R. Montgomery, S. Kothari, A. Castillo Castillo, R. Partelli, and L. Schroeder for comments in early versions of this manuscript.

Author Contribution

G.S. and A.S. designed the experiment. G.S. collected and analyzed the data with contributions from A.S. G.S. and A.S. wrote the manuscript.

618 **References**

619 Adams H.D., Zeppel M.J.B., Anderegg W.R.L., Hartmann H., Landhäusser S.M., Tissue D.T., …
620 McDowell N.G. (2017) A multi-species synthesis of physiological mechanisms in drought-
621 induced tree mortality. *Nature Ecology & Evolution* **1**, 1285–1291.

622 Allen C.D., Breshears D.D. & McDowell N.G. (2015) On underestimation of global vulnerability to
623 tree mortality and forest die-off from hotter drought in the Anthropocene. *Ecosphere* **6**, 1–
624 55.

625 Anderegg W.R.L., Berry J.A. & Field C.B. (2012) Linking definitions, mechanisms, and modeling of
626 drought-induced tree death. *Trends in Plant Science* **17**, 693–700.

627 Asner G.P., Brodrick P.G., Anderson C.B., Vaughn N., Knapp D.E. & Martin R.E. (2015) Progressive
628 forest canopy water loss during the 2012–2015 California drought. *Proceedings of the*
629 *National Academy of Sciences* **2015**, 201523397.

630 Barigah T.S., Charrier O., Douris M., Bonhomme M., Herbette S., Améglio T., … Cochard H. (2013)
631 Water stress-induced xylem hydraulic failure is a causal factor of tree mortality in beech and
632 poplar. *Annals of Botany* **112**, 1431–1437.

633 Barrs H.D. & Weatherley P.E. (1962) A Re-Examination of the Relative Turgidity Technique for
634 Estimating Water Deficits in Leaves. *Australian Journal of Biological Sciences* **15**, 413–428.

635 Bartlett M.K., Scoffoni C. & Sack L. (2012) The determinants of leaf turgor loss point and prediction
636 of drought tolerance of species and biomes: a global meta-analysis. *Ecology Letters* **15**, 393–
637 405.

638 Begg J.E. & Turner N.C. (1970) Water Potential Gradients in Field Tobacco. *Plant Physiology* **46**,
639 343–346.

640 Blackman C.J., Pfautsch S., Choat B., Delzon S., Gleason S.M. & Duursma R.A. (2016) Toward an
641 index of desiccation time to tree mortality under drought. *Plant Cell and Environment* **39**,
642 2342–2345.

643 Boyer J.S., James R.A., Munns R., Condon T. & Passioura J.B. (2008) Osmotic adjustment leads to
644 anomalously low estimates of relative water content in wheat and barley. *Functional Plant*
645 *Biology* **35**, 1172–1182.

646 Brodribb T.J. & Cochard H. (2009) Hydraulic failure defines the recovery and point of death in
647 water-stressed conifers. *Plant physiology* **149**, 575–84.

648 Carrer M., Von Arx G., Castagneri D. & Petit G. (2014) Distilling allometric and environmental
649 information from time series of conduit size: The standardization issue and its relationship to
650 tree hydraulic architecture. *Tree Physiology* **35**, 27–33.

651 Ceccato P., Flasse S., Tarantola S., Jacquemoud S. & Grégoire J.M. (2001) Detecting vegetation leaf
652 water content using reflectance in the optical domain. *Remote Sensing of Environment* **77**,
653 22–33.

654 Choat B., Jansen S., Brodribb T.J., Cochard H., Delzon S., Bhaskar R., … Zanne A.E. (2012) Global
655 convergence in the vulnerability of forests to drought. *Nature* **491**, 752–755.

656 Cochard H., Badel E., Herbette S., Delzon S., Choat B. & Jansen S. (2013) Methods for measuring

plant vulnerability to cavitation: a critical review. *Journal of Experimental Botany* **64**, 4779–4791.

Cohen Y., Alchanatis V., Meron M., Saranga Y. & Tsipris J. (2005) Estimation of leaf water potential by thermal imagery and spatial analysis. *Journal of Experimental Botany* **56**, 1843–1852.

Cregg B.M. (1994) Carbon allocation, gas exchange, and needle morphology of Pinus ponderosa genotypes known to differ in growth and survival under imposed drought. *Tree Physiology* **14**, 883–898.

Dai A. (2013) Increasing drought under global warming in observations and models. *Nature Climate Change* **3**, 52–58.

Daubenmire R.F. (1972) Phenology and other characteristics of tropical semi-deciduous forest in north-western Costa Rica. *The Journal of Ecology* **60**, 147–170.

Delzon S., Douthe C., Sala A. & Cochard H. (2010) Mechanism of water-stress induced cavitation in conifers: bordered pit structure and function support the hypothesis of seal capillary-seeding. *Plant, Cell & Environment* **33**, 2101–2111.

Elsayed S., Darwish W., Elsayed S. & Darwish W. (2017) Hyperspectral remote sensing to assess water status, biomass and yield ofmaize cultivars under salinity and water stress. **76**, 62–7262.

Espino S. & Schenk H.J. (2011) Mind the bubbles: Achieving stable measurements of maximum hydraulic conductivity through woody plant samples. *Journal of Experimental Botany* **62**, 1119–1132.

Fontes C.G. & Cavender-Bares J. (2019) Toward an integrated view of the "elephant": Unlocking the mysteries of water transport and xylem vulnerability in oaks. *Tree Physiology*.

Galiano L., Martínez-Vilalta J., Sabaté S. & Lloret F. (2012) Determinants of drought effects on crown condition and their relationship with depletion of carbon reserves in a Mediterranean holm oak forest. *Tree Physiology* **32**, 478–489.

Garcia-Forner N., Sala A., Biel C., Savé R. & Martínez-Vilalta J. (2016) Individual traits as determinants of time to death under extreme drought in Pinus sylvestris L. *Tree Physiology* **36**, 1196–1209.

Greenwood S., Ruiz-Benito P., Martínez-Vilalta J., Lloret F., Kitzberger T., Allen C.D., … Jump A.S. (2017) Tree mortality across biomes is promoted by drought intensity, lower wood density and higher specific leaf area. *Ecology Letters* **20**, 539–553.

Gregorczyk A. (1998) Richards plant growth model. *Journal of Agronomy and Crop Science* **181**, 243–247.

Guadagno C.R., Ewers B.E., Speckman H.N., Aston T.L., Huhn B.J., DeVore S.B., … Weinig C. (2017) Dead or alive? Using membrane failure and chlorophyll fluorescence to predict mortality from drought. *Plant Physiology* **175**, 223–234.

Guisan A. & Zimmermann N.E. (2000) Predictive habitat distribution models in ecology. *Ecological Modelling*.

Hacke U.G. & Sperry J.S. (2001) Functional and ecological xylem anatomy. *Perspectives in Plant*

Ecology, Evolution and Systematics **4**, 97–115.

Hacke U.G., Sperry J.S., Ewers B.E., Ellsworth D.S., Schäfer K.V.R. & Oren R. (2000) Influence of soil porosity on water use in Pinus taeda. *Oecologia* **124**, 495–505.

Hammond W.M., Adams H.D., Yu K., Wilson L.A., Will R.E. & Anderegg W.R.L. (2019) Dead or dying? Quantifying the point of no return from hydraulic failure in drought-induced tree mortality. *New Phytologist* **223**, 1834–1843.

Hastings S., Oechel W. & Sionit N. (1989) *Water relations and photosynthesis of chap- arral resprouts and seedlings following fire and hand clearing*. (ed K. SC), Natural History Museum of Los Angeles County, Los Angeles.

Hoch G., Popp M. & Körner C. (2002) Altitudinal increase of mobile carbon pools in Pinus cembra suggests sink limitation of growth at the Swiss treeline. *Oikos* **98**, 361–374.

Hoffmann W. a., Marchin R.M., Abit P. & Lau on L. (2011) Hydraulic failure and tree dieback are associated with high wood density in a temperate forest under extreme drought. *Global Change Biology* **17**, 2731–2742.

Kaufmann M. (1968) Evaluation of the Pressure Chamber Technique for Estimating Plant Water Potential of Forest Tree Species. *Forest Science* **14**, 369–374.

Konings A.G., Yu Y., Xu L., Yang Y., Schimel D.S. & Saatchi S.S. (2017) Active microwave observations of diurnal and seasonal variations of canopy water content across the humid African tropical forests. *Geophysical Research Letters* **44**, 2290–2299.

Maherali H. & DeLucia E.H. (2000) Xylem conductivity and vulnerability to cavitation of ponderosa pine growing in contrasting climates. *Tree Physiology* **20**, 859–867.

Maherali H. & Pockman W.T. (2004) Adaptive Variation in the Vulnerability of Woody Plants To Xylem Cavitation. *Ecology* **85**, 2184–2199.

Mardia K. V., Kent J.T. & Bibby J.M. (1979) *Multivariate Analysis*. Academic Press.

Martinez-Vilalta J., Anderegg W.R.L., Sapes G. & Sala A. (2019) Greater focus on water pools may improve our ability to understand and anticipate drought-induced mortality in plants. *New Phytologist* **223**, 22–32.

Martinez-Vilalta J., Sala A. & Pinol J. (2004) The hydraulic architecture of Pinaceae. *Plant Ecology* **171**, 3–13.

Marusig D., Petruzzellis F., Tomasella M., Napolitano R., Altobelli A. & Nardini A. (2020) Correlation of Field-Measured and Remotely Sensed Plant Water Status as a Tool to Monitor the Risk of Drought-Induced Forest Decline. *Forests* **11**, 77.

Matías L., González-Díaz P. & Jump A.S. (2014) Larger investment in roots in southern range-edge populations of Scots pine is associated with increased growth and seedling resistance to extreme drought in response to simulated climate change. *Environmental and Experimental Botany* **105**, 32–38.

Mcculloh K.A., Johnson D.M., Meinzer F.C. & Woodruff D.R. (2014) The dynamic pipeline: Hydraulic capacitance and xylem hydraulic safety in four tall conifer species. *Plant, Cell and Environment* **37**, 1171–1183.

Meinzer F.C., Woodruff D.R., Marias D.E., Smith D.D., McCulloh K.A., Howard A.R. & Magedman A.L. (2016) Mapping 'hydroscapes' along the iso- to anisohydric continuum of stomatal regulation of plant water status. *Ecology Letters*.

Mencuccini M., Minunno F., Salmon Y., Martínez-Vilalta J. & Hölttä T. (2015) Coordination of physiological traits involved in drought-induced mortality of woody plants. *New Phytologist* **208**, 396–409.

Mirzaie M., Darvishzadeh R., Shakiba A., Matkan A.A., Atzberger C. & Skidmore A. (2014) Comparative analysis of different uni- and multi-variate methods for estimation of vegetation water content using hyper-spectral measurements. *International Journal of Applied Earth Observation and Geoinformation* **26**, 1–11.

Mischan M.M., Pinho S.Z. de & Carvalho L.R. de (2011) Determination of a point sufficiently close to the asymptote in nonlinear growth functions. *Scientia Agricola* **68**, 109–114.

Mitchell P.J., O'Grady A.P., Tissue D.T., White D. a., Ottenschlaeger M.L. & Pinkard E. a. (2013) Drought response strategies define the relative contributions of hydraulic dysfunction and carbohydrate depletion during tree mortality. *New Phytologist* **197**, 862–872.

Nardini A., Petruzzellis F., Marusig D., Tomasella M., Natale S., Altobelli A., … Zini L. (2020) Water 'on the rocks': a summer drink for thirsty trees? *New Phytologist*, 1–14.

O'Brien M.J., Leuzinger S., Philipson C.D., Tay J. & Hector A. (2014) Drought survival of tropical tree seedlings enhanced by non-structural carbohydrate levels. *Nature Climate Change* **4**, 1–5.

Olson M.E., Soriano D., Rosell J.A., Anfodillo T., Donoghue M.J., Edwards E.J., … Méndez-Alonzo R. (2018) Plant height and hydraulic vulnerability to drought and cold. *Proceedings of the National Academy of Sciences* **115**, 7551–7556.

Padilla F. & Pugnaire F. (2016) Rooting Depth and Soil Moisture Control Mediterranean Woody Seedling Survival during Drought. *Functional Ecology* **21**, 489–495.

Piñol J. & Sala a. (2000) Ecological implications of xylem cavitation for several Pinaceae in the Pacific Northern USA. *Functional Ecology* **14**, 538–545.

Potter K.M., Hipkins V.D., Mahalovich M.F. & Means R.E. (2013) Mitochondrial DNA haplotype distribution patterns in Pinus ponderosa (Pinaceae): Range-wide evolutionary history and implications for conservation. *American Journal of Botany* **100**, 1562–1579.

Quentin A.G., Pinkard E.A., Ryan M.G., Tissue D.T., Baggett L.S., Adams H.D., … Woodruff D.R. (2015) Non-structural carbohydrates in woody plants compared among laboratories. *Tree Physiology* **35**, 1146–1165.

R Core Team (2020) R: A language and environment for statistical computing.

Rao K., Anderegg W.R.L., Sala A., Martínez-Vilalta J. & Konings A.G. (2019) Satellite-based vegetation optical depth as an indicator of drought-driven tree mortality. *Remote Sensing of Environment* **227**, 125–136.

Saatchi S., Asefi-Najafabady S., Malhi Y., E. O. C. Aragão L., Anderson L.O., Myneni R.B. & Nemani R. (2013) Persistent effects of a severe drought on Amazonian forest canopy. *Proceedings of the National Academy of Sciences* **110**, 565–570.

Sanders G.J. & Arndt S.K. (2012) Osmotic Adjustment Under Drought Conditions. In *Plant Responses to Drought Stress*. pp. 199–229. Springer Berlin Heidelberg, Berlin, Heidelberg.

Sapes G., Demaree P., Lekberg Y. & Sala A. (2020) Plant carbohydrate depletion impairs water relations and spreads via ectomycorrhizal networks. *New Phytologist*, Accepted.

Sapes G., Roskilly B., Dobrowski S., Maneta M., Anderegg W.R.L., Martinez-Vilalta J. & Sala A. (2019) Plant water content integrates hydraulics and carbon depletion to predict drought-induced seedling mortality. *Tree Physiology* **39**, 1300–1312.

Sergent A.-S., Bréda N., Sanchez L., Bastein J.-C. & Rozenberg P. (2014) Coastal and interior Douglas-fir provenances differ in growth performance and response to drought episodes at adult age. *Annals of Forest Science* **71**, 709–720.

Sevanto S., McDowell N.G., Dickman L.T., Pangle R. & Pockman W.T. (2014) How do trees die? A test of the hydraulic failure and carbon starvation hypotheses. *Plant, cell & environment* **37**, 153–61.

Simeone C., Maneta M.P., Holden Z.A., Sapes G., Sala A. & Dobrowski S.Z. (2019) Coupled ecohydrology and plant hydraulics modeling predicts ponderosa pine seedling mortality and lower treeline in the US Northern Rocky Mountains. *New Phytologist* **221**, 1814–1830.

Sperry J.S., Donnelly J.R. & Tyree M.T. (1988) A method for measuring hydraulic conductivity and embolism in xylem. *Plant, Cell & Environment* **11**, 35–40.

Sperry J.S. & Love D.M. (2015) Tansley review What plant hydraulics can tell us about responses to climate-change droughts.

Stout D.L. & Sala A. (2003) Xylem vulnerability to cavitation in Pseudotsuga menziesii and Pinus ponderosa from contrasting habitats. *Tree Physiology*, 43–50.

Subbarao G.V., Nam N.H., Chauhan Y.S. & Johansen C. (2000) Osmotic adjustment, water relations and carbohydrate remobilization in pigeonpea under water deficits. *Journal of Plant Physiology* **157**, 651–659.

Tognetti R., Michelozzi M. & Giovannelli a (1997) Geographical variation in water relations, hydraulic architecture and terpene composition of Aleppo pine seedlings from Italian provenances. *Tree Physiology* **17**, 241–250.

Torres-Ruiz J.M., Jansen S., Choat B., McElrone A.J., Cochard H., Brodribb T.J., … Delzon S. (2015) Direct X-Ray Microtomography Observation Confirms the Induction of Embolism upon Xylem Cutting under Tension. *Plant Physiology* **167**, 40–43.

Torres-Ruiz J.M., Sperry J.S. & Fernández J.E. (2012) Improving xylem hydraulic conductivity measurements by correcting the error caused by passive water uptake. *Physiologia Plantarum* **146**, 129–135.

Trenberth K.E., Dai A., Van Der Schrier G., Jones P.D., Barichivich J., Briffa K.R. & Sheffield J. (2014) Global warming and changes in drought. *Nature Climate Change* **4**, 17–22.

Trifilo P., Barbera P.M., Raimondo F., Nardini A. & Gullo M. a. L. (2014) Coping with drought-induced xylem cavitation: coordination of embolism repair and ionic effects in three Mediterranean evergreens. *Tree Physiology* **34**, 109–122.

Tyree M.T., Engelbrecht B.M.J., Vargas G., Kursar T. a, States U., Forest A., … Vermont M.T.T. (2003) Desiccation Tolerance of Five Tropical Seedlings in Panama. Relationship to a Field Assessment of Drought Performance. *Plant physiology* **132**, 1439–1447.

Tyree M.T. & Sperry J.S. (1989) Vulnerability of Xylem to Cavitation and Embolism. *Ann. Rev. Plant. Phys. Mol. Bio.* **40**, 19–38.

Tyree M.T., Vargas G., Engelbrecht B.M.J. & Kursar T. a (2002) Drought until death do us part: a case study of the desiccation-tolerance of a tropical moist forest seedling-tree, Licania platypus (Hemsl.) Fritsch. *Journal of experimental botany* **53**, 2239–2247.

Ullah S., Skidmore A.K., Naeem M. & Schlerf M. (2012) An accurate retrieval of leaf water content from mid to thermal infrared spectra using continuous wavelet analysis. *Science of the Total Environment* **437**, 145–152.

Umaña M. & Swenson N. (2019) Does trait variation within broadly distributed species mirror patterns across species? A case study in Puerto Rico. **100**, 1–11.

Venturas M.D., Sperry J.S., Love D.M., Frehner E.H., Allred M.G., Wang Y. & Anderegg W.R.L. (2018) A stomatal control model based on optimization of carbon gain versus hydraulic risk predicts aspen sapling responses to drought. *New Phytologist*.

Walker S.H. & Duncan D.B. (1967) Estimation of the probability of an event as a function of several independent variables. *Biometrika*.

Wang Q. & Li P. (2012) Identification of robust hyperspectral indices on forest leaf water content using PROSPECT simulated dataset and field reflectance measurements. *Hydrological Processes* **26**, 1230–1241.

Zhang Y., Zhou S., Gentine P. & Xiao X. (2019) Can vegetation optical depth reflect changes in leaf water potential during soil moisture dry-down events? *Remote Sensing of Environment* **234**, 1–10.

839 **Figure legends**

840 **Figure 1:** The third derivative (red curve) identifies the point of the mortality curve (teal curve) at
841 which mortality risk starts to suddenly increase (incipient mortality threshold) in response to
842 physiological decline. The incipient mortality threshold (red dot) appears in the third derivative as
843 a peak -maximum or minimum depending on the nature of the physiological predictor- near the
844 wet end of the range of physiological values. Once the incipient mortality threshold is identified,
845 we can evaluate the probability of mortality at which such threshold occurs (red dashed line) and
846 determine the degree of incipiency. The physiological value (X) of the incipient threshold can vary
847 among mortality curves of different organs and populations. Little variation among curves leads to
848 more consistent thresholds.

849 **Figure 2.** Morphological differences between North Plateau (NP) and Rocky Mountain (RM)
850 seedlings. NP seedlings were larger in size and biomass and allocated greater biomass to below
851 ground organs. Differences among populations are significant across all panels.

852 **Figure 3.** Changes in population-level mortality, drought intensity, and whole-plant physiological
853 status over time. Panel A: Water potentials decreased over time in soil (black), stem (yellow) and
854 leaves (green) but North Plateau (NP, circles and corresponding solid line) seedlings experienced
855 greater decline rates than Rocky Mountain (RM, crosses and corresponding dashed line) seedlings.
856 Panel B: Both populations experienced loss of conductivity over time in both stems and roots
857 (gray) and at the whole-plant level (purple), but NP seedlings lost hydraulic conductivity at faster
858 rates in all organs. Panel C: Non-structural carbohydrates declined over time in both populations,
859 but NP seedlings experienced greater root NSC depletion rates from day 29 onward. Panel D:
860 Relative water content declined over time at similar rates across all organs, but NP seedlings
861 dehydrated faster than RM seedlings. Panel E: Probability of mortality increased after day 29 and
862 42 of drought in NP and RM seedlings, respectively.

863 **Figure 4.** Degree of threshold incipiency, threshold consistency, and predictive power of each
864 predictor of mortality. Relative water content (RWC) and water potential predicted DIM risk in all
865 organs (gray: roots, yellow: stems, green: leaves, and purple: plant) and populations (circles: North
866 Plateau (NP), crosses: Rocky Mountain (RM)) and had a similar average predictive power (i.e.
867 variance explained), variability in predictive power, and threshold consistency. However, RWC
868 showed the most incipient thresholds. Non-structural carbohydrates (NSC) (black) were not able
869 to predict DIM risk from leaves, showed lower average predictive power and higher variability in

predictive power than RWC and water potential, less incipient thresholds, and the lowest threshold consistency. Percent loss of hydraulic conductivity (PLC) (orange) only predicted DIM risk in NP seedlings (circles) and had lower average predictive power even when excluding the RM population (crosses) to avoid potential effects of uncertainty in hydraulic conductivity measurements due to low flow rates caused by their small size. PLC ranked third in mortality threshold consistency and incipiency.

Figure 5. Relationships between DIM risk and each DIM predictor. Both relative water content (RWC) and water potential showed similar mortality functions with incipient mortality thresholds at turgor loss (vertical lines) across organs and populations. Percent loss conductivity (PLC) showed different mortality functions between NP (circles and corresponding solid lines) and RM seedlings (crosses and corresponding dashed lines) and no incipient mortality thresholds in RM seedlings. Mortality functions in NSC relative to control showed clear separation between NP and RM populations. NSC showed incipient mortality thresholds for roots (gray) and at the whole plant level (purple) but did not show thresholds in stems (yellow) and leaves (green) of RM seedlings. Note that black water potential curves correspond to soil water potential.

886 **Figures**

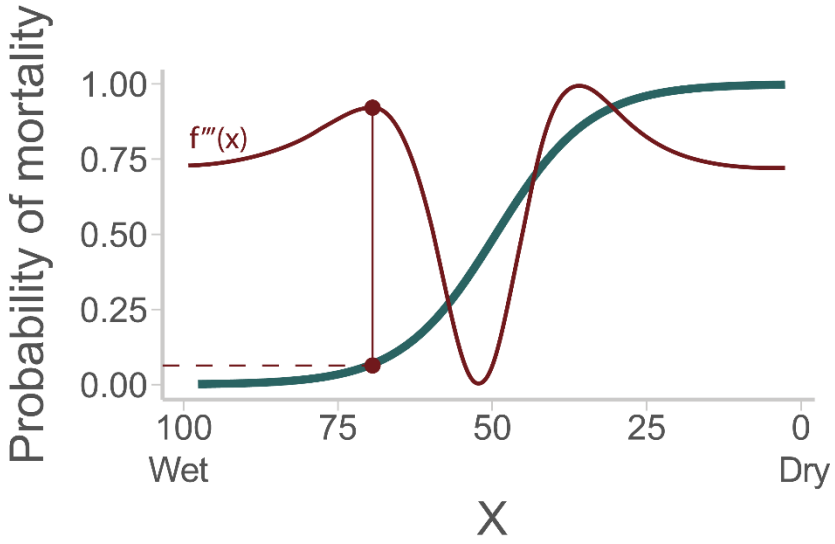

887

888 **Figure 1:** The third derivative (red curve) identifies the point of the mortality curve (teal curve) at
889 which mortality risk starts to suddenly increase (incipient mortality threshold) in response to
890 physiological decline. The incipient mortality threshold (red dot) appears in the third derivative as
891 a peak -maximum or minimum depending on the nature of the physiological predictor- near the
892 wet end of the range of physiological values. Once the incipient mortality threshold is identified,
893 we can evaluate the probability of mortality at which such threshold occurs (red dashed line) and
894 determine the degree of incipiency. The physiological value (X) of the incipient threshold can vary
895 among mortality curves of different organs and populations. Little variation among curves leads to
896 more consistent thresholds.

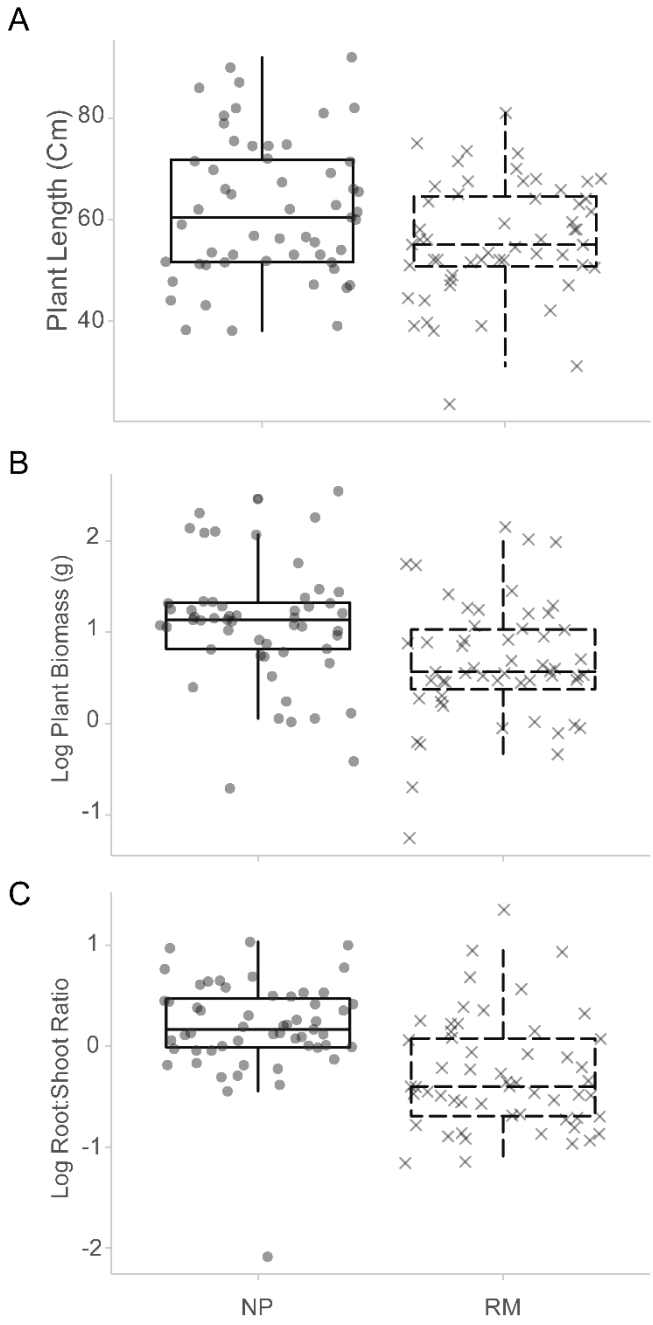

Figure 2. Morphological differences between North Plateau (NP) and Rocky Mountain (RM) seedlings. NP seedlings were larger in size and biomass and allocated greater biomass to below ground organs. Differences among populations are significant across all panels.

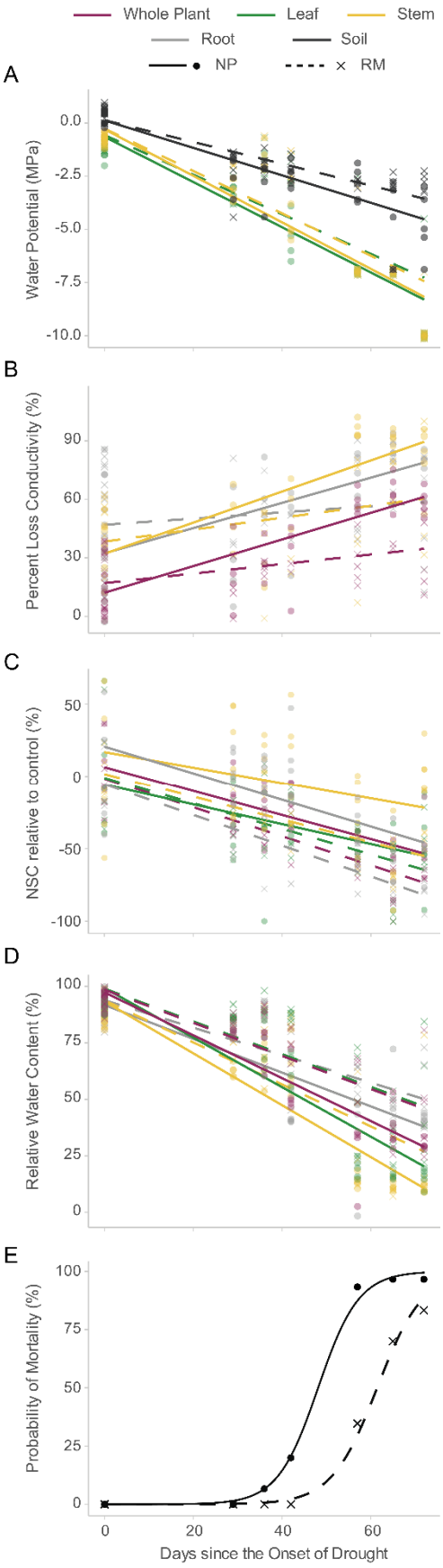
Whole Plant
Leaf
Stem
Root
Soil
NP
RM
A
Water Potential (MPa)
0.0
-2.5
-5.0
-7.5
-10.0
B
Percent Loss Conductivity (%)
90
60
30
0
C
NSC relative to control (%)
50
0
-50
-100
D
Relative Water Content (%)
100
75
50
25
0
E
Probability of Mortality (%)
100
75
50
25
0
0
20
40
60
Days since the Onset of Drought

902

903 **Figure 3.** Changes in population-level mortality, drought intensity, and whole-plant physiological
904 status over time. Panel A: Water potentials decreased over time in soil (black), stem (yellow) and
905 leaves (green) but North Plateau (NP, circles and corresponding solid line) seedlings experienced
906 greater decline rates than Rocky Mountain (RM, crosses and corresponding dashed line) seedlings.
907 Panel B: Both populations experienced loss of conductivity over time in both stems and roots
908 (gray) and at the whole-plant level (purple), but NP seedlings lost hydraulic conductivity at faster
909 rates in all organs. Panel C: Non-structural carbohydrates declined over time in both populations,
910 but NP seedlings experienced greater root NSC depletion rates from day 29 onward. Panel D:
911 Relative water content declined over time at similar rates across all organs, but NP seedlings
912 dehydrated faster than RM seedlings. Panel E: Probability of mortality increased after day 29 and
913 42 of drought in NP and RM seedlings, respectively.

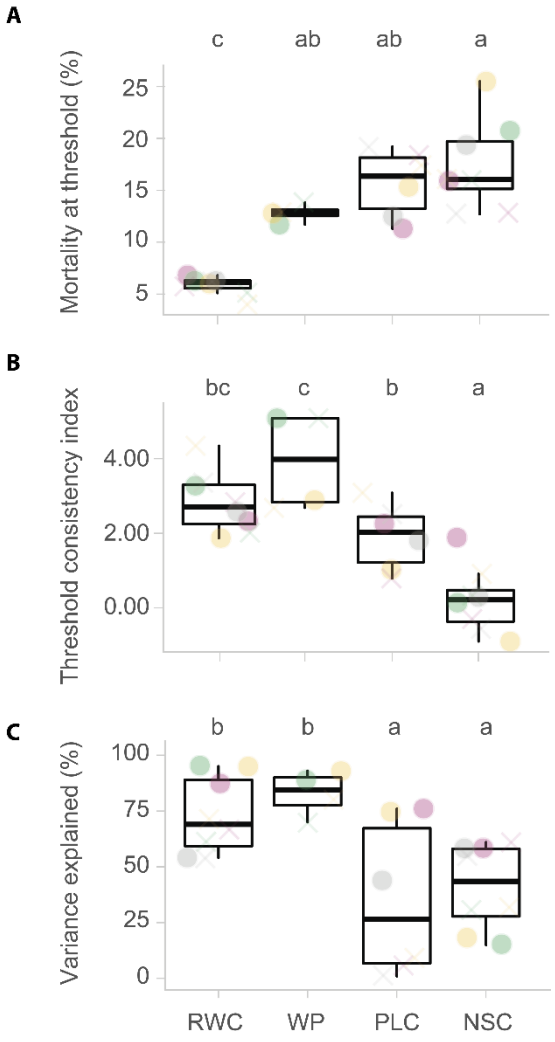

914

Figure 4. Degree of threshold incipiency, threshold consistency, and predictive power of each predictor of mortality. Relative water content (RWC) and water potential predicted DIM risk in all organs (gray: roots, yellow: stems, green: leaves, and purple: plant) and populations (circles: North Plateau (NP), crosses: Rocky Mountain (RM)) and had a similar average predictive power (i.e. variance explained), variability in predictive power, and threshold consistency. However, RWC showed the most incipient thresholds. Non-structural carbohydrates (NSC) (black) were not able to predict DIM risk from leaves, showed lower average predictive power and higher variability in predictive power than RWC and water potential, less incipient thresholds, and the lowest threshold consistency. Percent loss of hydraulic conductivity (PLC) (orange) only predicted DIM risk in NP seedlings (circles) and had lower average predictive power even when excluding the RM population (crosses) to avoid potential effects of uncertainty in hydraulic conductivity measurements due to low flow rates caused by their small size. PLC ranked third in mortality threshold consistency and incipiency.

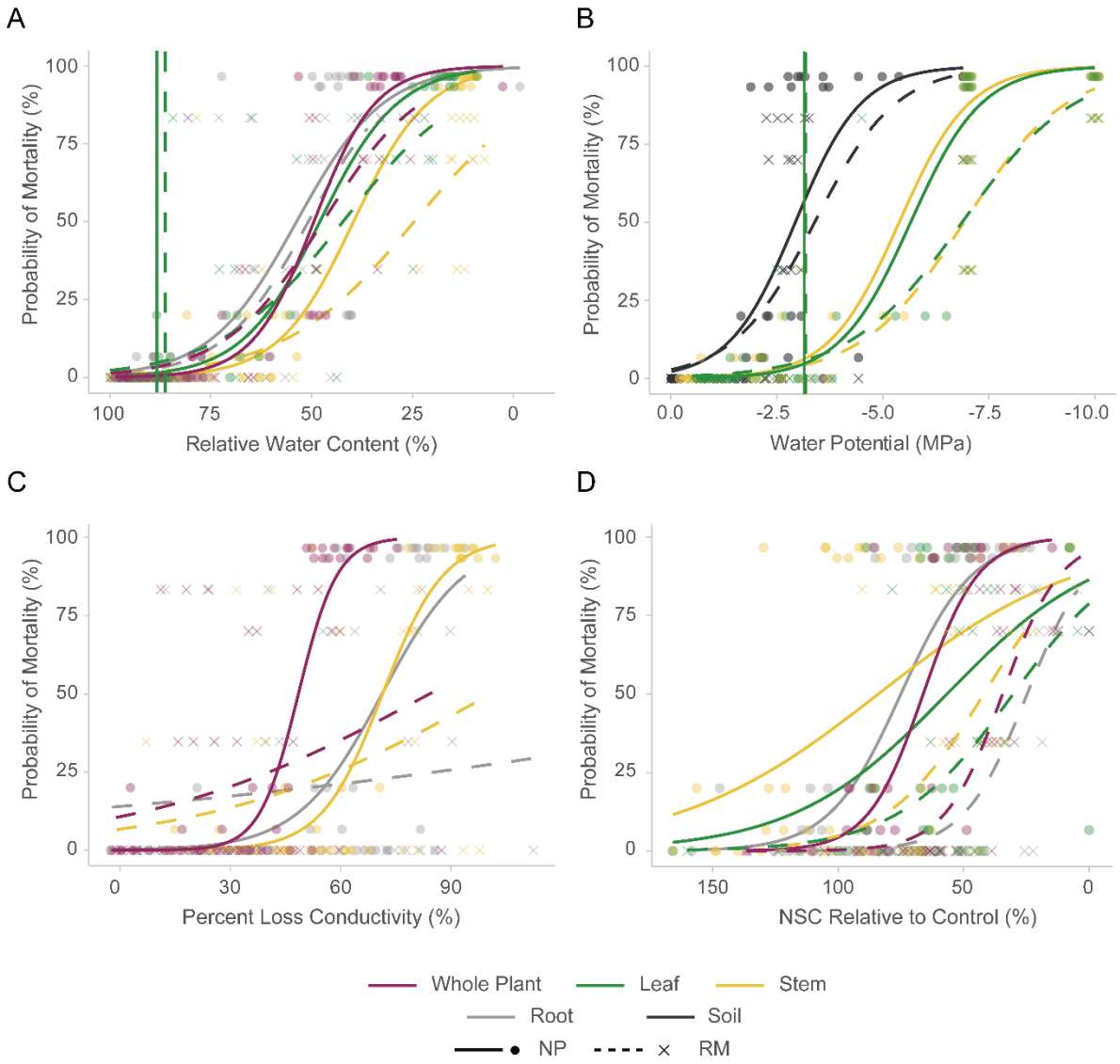

Figure 5. Relationships between DIM risk and each DIM predictor. Both relative water content (RWC) and water potential showed similar mortality functions with incipient mortality thresholds at turgor loss (vertical lines) across organs and populations. Percent loss conductivity (PLC) showed different mortality functions between NP (circles and corresponding solid lines) and RM seedlings (crosses and corresponding dashed lines) and no incipient mortality thresholds in RM seedlings. Mortality functions in NSC relative to control showed clear separation between NP and RM populations. NSC showed incipient mortality thresholds for roots (gray) and at the whole plant level (purple) but did not show thresholds in stems (yellow) and leaves (green) of RM seedlings. Note that black water potential curves correspond to soil water potential.